SOLAR MODULE ARC FAULT MODELING AT SANDIA NATIONAL LABORATORIES

Jason Strauch, Michael Quintana, Jennifer Granata, Ward Bower, Scott Kuszmaul
Sandia National Laboratories*
1515 Eubank Blvd SE
Albuquerque, NM 87123
jestrau@sandia.gov, 505-284-6114 ph., 505-284-67690 fax

ABSTRACT: Sandia Laboratories is performing modeling and analysis on the causes of solar arc fault failures and fires. As part of this work, recent module failures (modules ~6 years in service) at a large photovoltaic power plant in the southwest United States have been documented, and the failure modes determined through physics based analysis. The analysis and modeling indicates that arc faults within the module are likely the cause of the observed failures. Failed or failing solder connections between the busbars and connector ribbons, and connector ribbons and the backside contacts are the common theme in these failures. Electrical modeling shows that an interconnect ribbon to busbar connection that has separated by 5 microns (through either diurnal cycling or corrosion) can experience a sufficient electric field driven by just the module voltage, to cause an arc flash. Further thermo-mechanical modeling shows that a mere 0.4 mm^2 arc region can generate heat energy sufficient to shatter the glass, burn off (volatilize or boil) the copper busbar's tin coating, as well as char the other materials used in a solar module stack, all within the millisecond to 2 second time frame.

1 INTRODUCTION

Fires in solar photovoltaic (PV) systems have been in the news the last few years. As an industry without a long history, preventing these fires is of the utmost importance for public perception of the safety of solar PV. This will benefit the community (both global and solar) by allowing the greatest market penetration of renewable energy resources based on solar PV technology. As part of Sandia National Laboratories work in PV we are tasked with supporting the United States Department of Energy (DOE) and the solar industry in a wide variety of areas specific to PV.

These areas include, but are not limited to, fundamental research in solar cells and device physics, system modeling, grid distribution and transmission integration, safety and reliability testing and evaluation, and supporting the development of applicable codes and standards for entities such as the Underwriters Laboratory (UL) and National Electric Code (NEC).

The solar arc fault work at Sandia National Labs (SNL) is in direct support of safety and reliability testing and code development. The work described herein is specific to arc faults discovered in crystalline silicon modules at a large PV powerplant in Arizona. This powerplant has seen a number of module failures in recent years, and has provided Sandia (through the module manufacturer) with pictorial examples of these failed modules to analyze. The work described herein is specific to arc faults discovered in crystalline silicon modules with roughly 6 years of service at a large PV powerplant in Arizona.

The failed modules all have evidence of what appears to be burns on both sides of the module layup stack. Some modules suffered shattered front glass, with cracking that appears to originate above a burn spot. Another has shifted/deformed busbars and what appears to be broken interconnect ribbon-to-busbar contacts. The next section describes these in greater detail and also describes the set up for the analysis and modeling performed to explain these failures.

2 MODEL SET UP AND MODULE FAILURES

2.1 Physics Simulation Set Up

Accurate physics modeling of true multiphysics phenomena requires accurate geometry, material and boundary conditions for any system. A full scale module design with crystalline silicon cells and a standard stack including backside contacts and Tedlar, top and bottom EVA sheet and cell gridlines and collector is used for all Finite Element Analysis (FEA) and is shown in Figure 1.

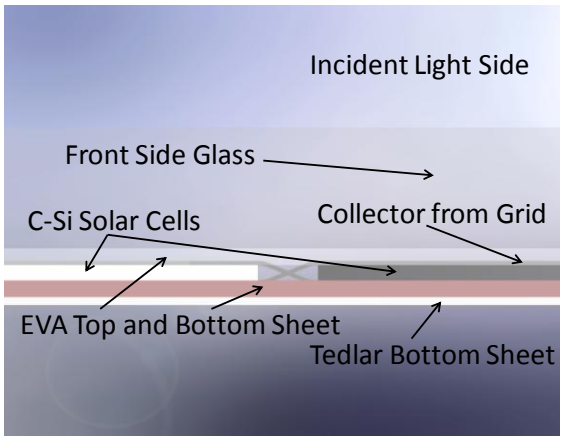

Figure 1: Solar Module Model Stack

The stack geometry and material properties determine the electrical and thermal characteristics of the system. The overall module model with the failure zones highlighted is shown in Figure 2 and described below.

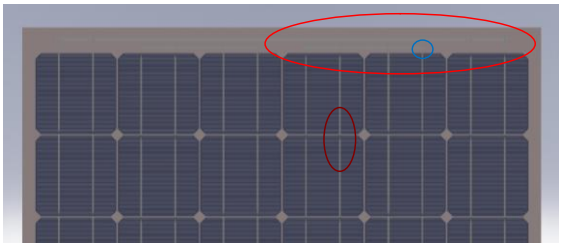

Figure 2: Full Module Model Showing Three Failure Zones

2.2 Observed Module Failures

All of the observed module failure locations had a brown and burned appearance. Three primary failures can be seen in the modules:

1. Busbar discoloration, which was prevalent in virtually all failures. Some had associated busbar shifting and bending.
2. Discoloration at the location that the interconnect ribbon goes from the cell back contact to the front side grid. Common.
3. Discoloration along the interconnect ribbon occurred along the edge of the cells as well as inboard, closer to the center of the cells
4. Front side glass cracked above burned spot.

These failure modes are shown in Figures 3 to 6.

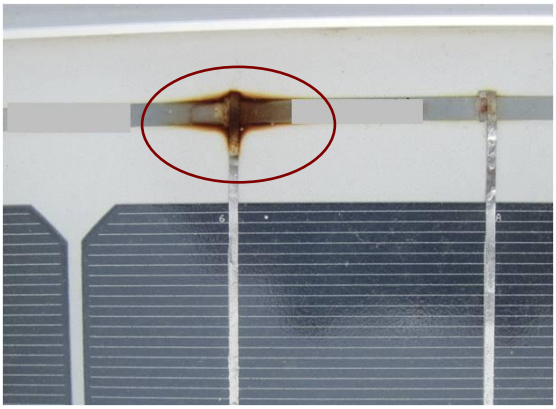

Figure 3: Collector Ribbon to Busbar Browning and Connection

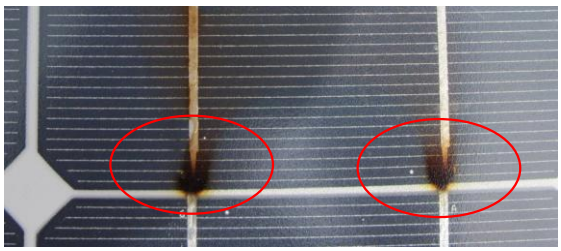

Figure 4: Collector Ribbon Front to Backside Discoloration

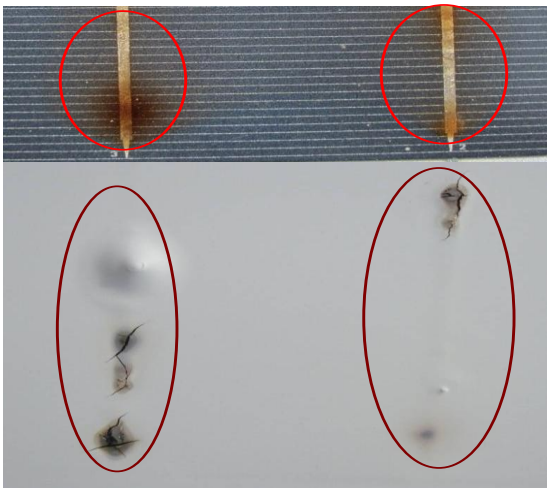

Figure 5: Front and backside views of damage where interconnect ribbons attach to the cell metallization

The failures shown in Figures 3 to 5 were analyzed according to electrostatic and thermo-mechanical first principle physics. Another case analyzed is a busbar discoloration with an associated glass fracture of the top glass in the module and is shown in Figure 6

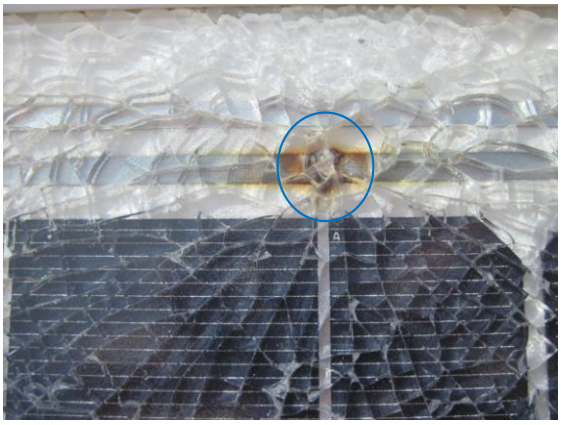

Figure 6: Ribbon to Busbar Burn Causing Glass Fracture

The first phenomenon analyzed was the conditions needed to cause an arc fault for a given geometry and input conditions. This and the other failure conditions are analyzed below.

3 ANALYSIS AND MODELING RESULTS

Using the full module model described in the prior section, various subdomains were analyzed according to the failures shown above. The electrical conditions to cause the most prevalent failure, the ribbon-to-busbar discoloration or burning is performed first. Assuming a 43.5 V open circuit voltage (Voc), a full contact area between the ribbon and the busbar was modeled to determine the gap needed to cause an arc fault (flash).

The electric field strength determines the force on the air ions between the electrodes. Once the electric field, and thus force on the ions is sufficient, they collide with other ions with sufficient force to create extra free electrons, which results in a cascade effect of dielectric breakdown, resulting in very high conductivity in the air gap, a formerly good insulator medium.

The movement of thermal energy within the module stack and laterally is governed by Fourier's Law of Conduction:

$$q = \frac{k \cdot A}{L}\left(T_{hot} - T_{cold}\right) \qquad \text{Eq. 1}$$

Fourier's Law states that the heat flow, q, is equal to the material conductivity, k, times the heat flow cross sectional area, A, divided by the length the heat transfer occurs over, times the temperature difference.

The thermal expansion is governed by the linear, area or volumetric expansion described by the basic formula below, Equation 2, which states the change in length due to a temperature change is equal to the original length times the coefficient of thermal expansion (CTE) times the temperature change. The change in length/area/volume exerts stress on surrounding areas as developed by Equation 3.

$$\Delta L = \alpha \cdot L \cdot \Delta T \qquad \text{Eq. 2}$$

Equation 2 can also be rearranged in terms of strain, which can be related to material stress as shown in the equations developed below. Stress is the pulling (or pushing) force divided by the cross sectional area.

$$\varepsilon = \frac{\Delta L}{L_0} = \alpha \cdot \Delta T$$

$$\sigma = \frac{F}{A_0} \qquad \sigma = E \cdot \varepsilon = E \cdot \alpha \cdot \Delta T$$

Eqs. 3

Here, ε is strain, E is the modulus of elasticity or stiffness of the material, and σ is the stress. Excessive stress or rate of application of stress is what causes materials to fail and break.

The differential forms of the above equations are solved discretely over very small elements using Solidworks Simulation Finite Element Analysis code.

3.1 Electrical Arc Flash Modeling

For this study, the subdomain selected needs to be small enough to account for a single micron thickness air or metal oxide gap in between two conductors that are at the module potential. The module stack is just under 6 mm thick, and the material subdomain measures 6.5 mm wide by 7.5 mm long. The area subject to an electrical gap (or corrosion buildup) is 2.54 mm (ribbon width) by 5.08 mm (busbar width). The subdomain mesh, which accounts for single micron range gaps, is shown in Figure 7.

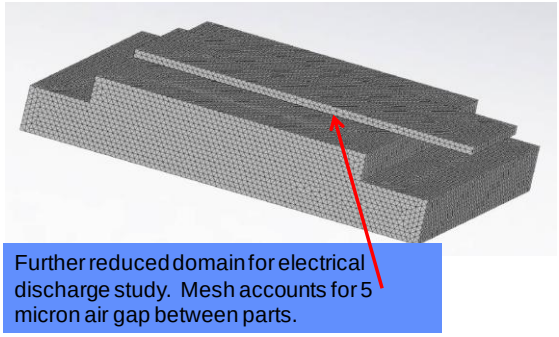

Figure 7: Busbar to ribbon electrical discharge subdomain mesh

Figure 8 shows the electric potential with the module's 43.5 V Voc applied between the busbar and ribbon with a 5 micron air gap.

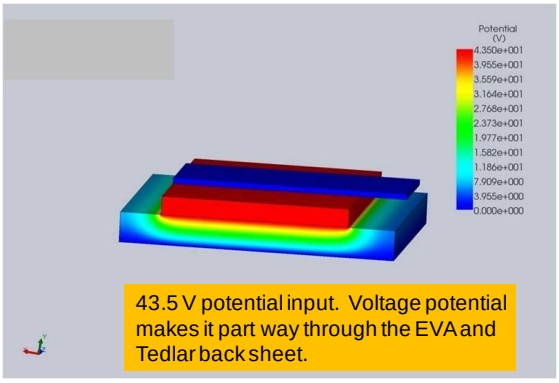

Figure 8: Module Voc applied across 5 micron gap between busbar and collector

The voltage potential across a gap of some dielectric medium (air was modeled in this case) will have a breakdown potential, above which the formerly insulating medium will become a very good conductor through ion mobility driven by the potential. For air the dielectric strength varies with pressure, and is about 3000 V/mm (75 V/mil) at normal atmospheric pressure [1], [2].

Dielectric breakdown occurs when a charge buildup exceeds the electrical limit or dielectric strength of a material. The negatively charged electrons are pulled in one direction and the positively charged ions in the opposite direction. When electrons are removed from a nucleus, the nucleus becomes positively charged. When air molecules become ionized in a very high electric field, the air changes from an insulator to a conductor. Sparks occur because of the recombination of electrons and ions. Lightning occurs when there is a buildup of charge on the clouds and the ground. It produces the electric field that exceeds the dielectric strength of air. Ionized air is a good conductor and provides a path whereby charges can flow from clouds to ground.

The dielectric strength of air is approximately 3 kV/mm. Exact value of the dielectric strength varies with the shape and size of the electrodes and increases with the pressure of the air.

The predicted electric field strength for a 5 micron gap with a 43.5 V potential across it is almost triple the dielectric strength of air, or about 8.7 kV/mm. With flat plate surfaces, the modeled joint readily exceeds the dielectric breakdown strength and an arc flash with possible sustained arcing can occur. The electric field strength developed across the busbar and connector ribbon is shown in Figure 9.

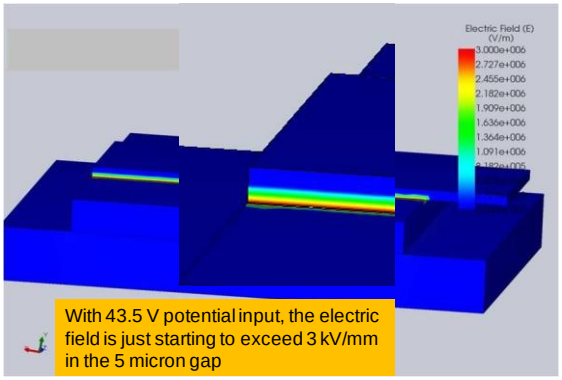

Figure 9: Electric Field Strength with Module Open Circuit Voltage Applied across a 5 micron gap

Once the geometric and material limits to dielectric breakdown have been determined, the extreme temperature an electrical arc generates can be modeled. The extreme temperature, frequently reported at 6000K and above, [3], [4] is enough to vaporize most metals. Most knowledge of high energy electric arcs comes from the arc welding industry.

3.2 Glass Fracture Analysis

The module with the glass fracture directly above a burned ribbon-to-busbar joint, shown in Figure 6, is analyzed next. This analysis was focused on both the temperature scale and time scale for the heating. For the glass fracture, a 40x40 mm subdomain through the thickness of the module stack, and centered over the burned busbar connection was modeled. Although the

breakdown was modeled over the entire area of the joint, it is likely that just a portion of the joint, perhaps one end, caused the burn. For this reason, the temperature input, 6000K, for the glass fracture model was applied on just the 0.4 mm^2 area of the end of the interconnect.

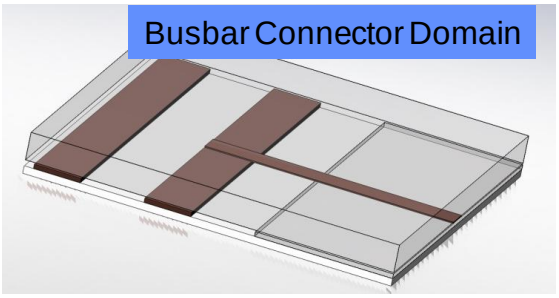

Figure 10: Glass Fracture Busbar Domain

Even with such a small arc area, due to the extreme temperatures generated in the arc plasma, the time scale for heating the module stack is very short. After just 200 milliseconds the copper on the arc surfaces of the busbar and connector ribbon is 1200K, at which point the copper is about to melt and the tin coating has already failed. After 2 seconds of arcing, the glass stack has absorbed enough heat energy fast enough to exceed the modulus of rupture of the tempered, textured front side glass. The temperature distribution is shown in Figure 11.

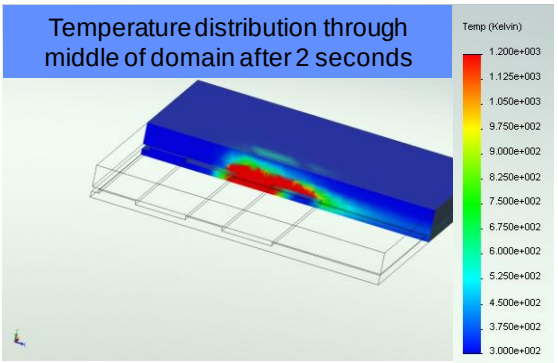

Figure 11: Arc Induced Module Temperature within seconds of Initiation

The front glass breaks when the temperature induced state of stress, due to localized expansion near the arc, exceeds the modulus of rupture of the glass. Flabeg quotes the modulus of rupture of their tempered glass as 120 MPa and 90 MPa with a stipple pattern. Other manufacturers of solar glass, such as Saint Gobain, quote similar values for tempered and less for float glass or simply heat strengthened. The Modulus of Rupture for the Finite Element Analysis was assumed to be 100 MPa, though changes in this value will just change the time to rupture. The state of stress for the module stack and glass are shown in Figure 12.

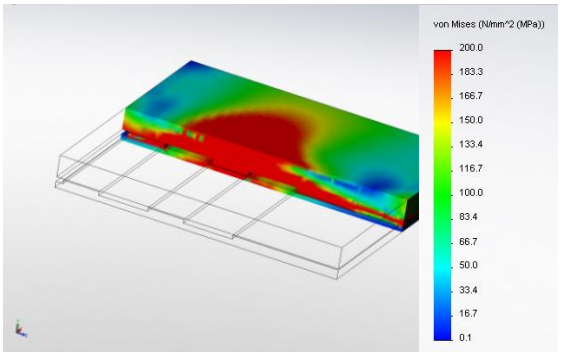

Figure 12: Glass Stress after 2 seconds of arcing exceeds the rupture strength by 100%

The heat of the arcing expands the glass region directly above the arc, putting the immediate surrounding area into tension, resulting in the radial break pattern. Since the glass is tempered, the entire pane fractures into small pieces.

3.3 Busbar Burning and Displacement Analysis

On another failed module the busbar to connector ribbon appeared burned and the busbar appears to have shifted permanently within the layup stack.

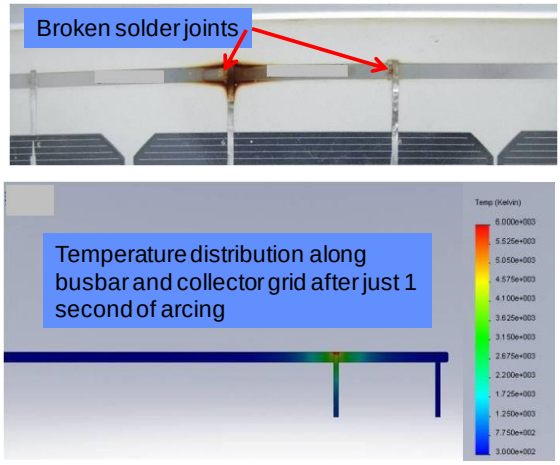

Figure 13:Busbar arc temperature distribution after 1 second

Applying the 6000K temperature heat load to the busbar structure as in the prior analysis, and calculating the displacement due to the thermal expansion shows that it is plausible that the busbars were deformed in the module stack by the arc that burned the connection. This is shown in Figure 14.

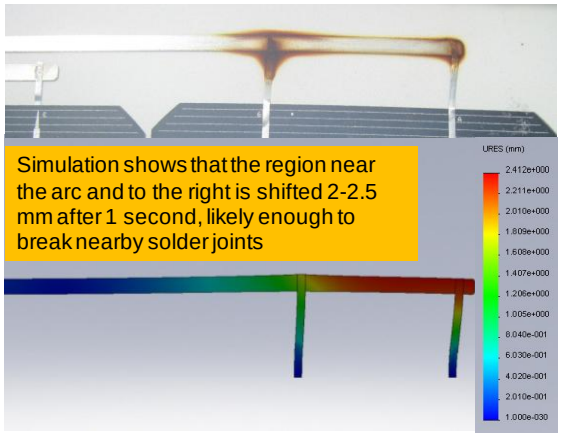

Figure 14: Busbar Deformation due to arc heating

3.4 Backside Contact Burns and Fabrication Issues

The final failure mode, interconnect ribbon burning in the mid-region of cells was not investigated. Based on the thermo-electrical modeling of the other failures, it is likely that high temperatures generated by arcing caused the burns. What isn't known is whether the arcing was due to interconnect ribbon to grid line contact problems or interconnect ribbon to backside contact on the cells. The Tedlar and EVA charring appears more severe on the backside of these mid cell failures, as may be seen in Figure 5 in Section 2.2. The figure below shows that more than one technique was used to create cell strings. Soldering cells into strings requires controlled time, temperature and pressure. It appears that the areas of the modules that were assembled with a roller process were more susceptible to poor contacts and the associated arc faults between the ribbons and the cells.

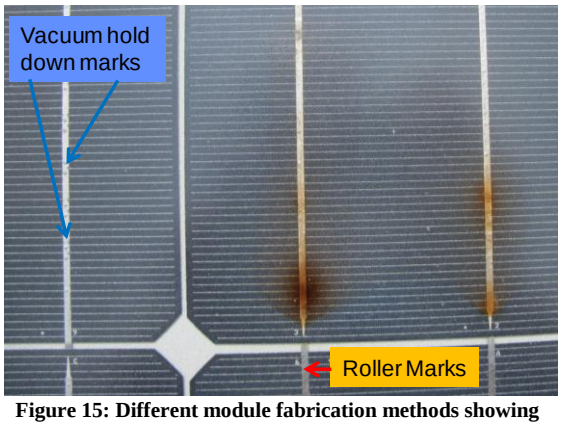

Figure 15: Different module fabrication methods showing arcing in the roller section

A major location of the arc fault failures is the inteconnect ribbon where it connects the top side grid lines to the next cell's backside contact. This can be seen in Figure 4 in Section 2.2. A side view of this feature created for the model is shown below.

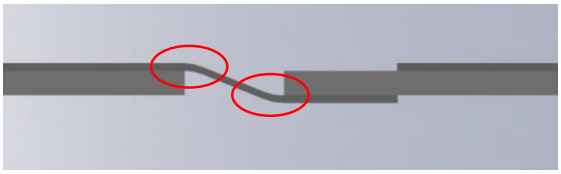

Figure 16: Side section of top to bottom contact failure region

These failures were not studied but the belief is that these common failures are related to the variations in fabrication method described above, combined with diurnal cycling of the module.

4 CONCLUSION AND FUTURE WORK

4.1 Conclusion

Physics based analysis and models were developed and used to solve for the conditions needed to cause the observed failures. Most of the failures analyzed can be explained by the high temperatures generated in the short time frames as would happen in electrical arc discharge. The cause of the arc faults is not readily discernible by this analysis. Analysis and testing of the failed modules will provide additional information and possibly identification of failure mode(s).

4.2 Future Work

Failure analysis of sample modules is planned. Non-destructive tests including outdoor electrical performance, dark IV, IR, ultrasound, and micro-Xray will be used to understand module state prior conducting destructive test. A coring technique developed at Sandia National Laboratories will be used to extract samples that will then be used for multiple materials tests. It is expected that these tests well help to confirm temperatures that caused failures. Further work in testing module materials to determine the dielectric strength of module materials to further improve the modeling capability is also planned.

5 REFERENCES

[1] P.A. Tipler, College Physics. Worth, 1987: 467.
[2] J.S. Rigden, Macmillan Encyclopedia of Physics, Simon&Schuster, 1996:353.
[3] B.H. Cary, Modern Welding Technology. Upper Saddle River. Prentice Hall, 1998: 466, 108.
[4] W.A. Bowditch, Welding Technology Fundamentals. Tinley park: the Goodheart-Wilcox Company, Inc. 1997: 269.

*Sandia is a multiprogram laboratory operated by Sandia Corporation, a Lockheed Martin Company, for the United States Department of Energy's National Nuclear Security Administration under Contract DE-AC04-94AL85000.